Journal of Applied Geophysics, 31 (1994) 145–152
Elsevier Science B.V., Amsterdam

Numerical simulation of radon transport from subsurface to buildings

T. Kohl, F. Medici and L. Rybach
Institut für Geophysik, ETH Zürich, Switzerland

(Received February 20, 1993; accepted after revision April 16, 1993)

ABSTRACT

The finite element code FRACTure was conceived for the simulation of forced fluid flow in fractured rock. For the treatment of radon transport through the subsurface only minor changes were necessary in this code (extension by a radioactive decay term). The calculations performed so far simulate steady state pressure and radon concentration fields in the ground surrounding a cylindrical building. Comparisons of numerical and analytic calculations for a simple geometry show excellent agreement.

Successive simulations demonstrate the significance of individual transport mechanisms. All models assume constant underpressure in the building and the validity of Darcy's law for mass transport in the underground as well as Fick's law for molecular dispersion.

The results show that the radon transport by advection and by diffusion strongly depends on the gas permeability of the underground. The source region of indoor radon extends over a limited volume of a few meters only. In soils with low permeability the diffusive flux is dominating even at high pressure differences between the building interior and the subsurface. In these cases the radiation risk due to radon entry is small. On the other hand a high soil gas permeability leads to a strong increase in radon entry into the building. For these advective dominated regimes even small pressure changes produce large changes in the indoor radon content.

Introduction

Because the awareness for possible health risk by environmental radioactivity developed only in the last 10–20 years, systematic studies on indoor radon concentrations have been performed only recently. These studies were mostly focused on the research of material properties and data acquisition, in order to understand the origin of indoor radon (Sögaard-Hansen and Damkjær, 1987; Nero, in: Nazaroff and Nero, 1988, pp. 1–56). Very few attemps have been made to quantitatively compute the radon transport from subsurface to buildings.

A computation with a semi-analytical approach was presented by Nazaroff and Sextro (1989), who calculated the radon entry into a buried cylinder with a horizontal axis. This cylinder is an idealisation of the main entry of radon in a building that might be a floor-wall joint or a perimeter drain tile system. By calculating the travel time of individual air flow pathways from the surface air to the cylinder they predict the radon entry rate in a building.

A fully numerical analysis of the problem was presented by Loureiro et al. (1990) who developed a 3-D finite difference code that was especially conceived for this purpose. For the first time a tool was available to calculate quantitatively the steady state radon entry in buildings. However, this code contains very strict geometrical limitations and is restricted to simulate steady state problems.

Apart from a numerical 2-D steady state calculation, Andersen (1992) was the first to perform an evaluation of the transient effects of indoor radon. He compared solutions of theo-

0926-9851/94/$07.00
SSDI 0926-9851(93)E0026-6

retically derived transfer functions with experimental data in order to study the coupling of an air pressure variation between a building and the surrounding underground.

In this paper a new approach for modelling radon transport processes will be presented. An existing coupled three-dimensional transient Finite Element code, named FRACTure (Kohl, 1992), was extended to the treatment of radon transport problems. This procedure offers all advantages of the finite element scheme, including the selection of geometry and materials as well as the use of a standard graphical presentation of the results. For future use transient datasets of radon entry can be simulated as well.

Radon transport mechanisms

At present it is understood that the source region of indoor radon is limited to some meters below the building. The physical mechanisms that are responsible for the radon transport from subsurface to buildings were described in detail by Nazaroff (1992). In the following section these mechanisms will be only briefly presented; the notations are described in Appendix 1.

Radon (Rn) is a radioactive gas with three naturally occurring isotopes that can flow in air pore space of the subsurface and is subject to radioactive decay. The half-life for ^{222}Rn is 3.8 days, for ^{220}Rn 55 s and for ^{219}Rn 4 s, respectively. Due to their very fast decay, ^{220}Rn and ^{219}Rn can only exceptionally cause radiation exposure problems. Therefore, in the following the term "radon" refers always to ^{222}Rn.

Radon is generated in the subsurface. The generation rate in a dry (not water saturated) underground is given by:

$$G = f\rho_s A_{Ra}\lambda(1-\epsilon)/\epsilon \qquad (1)$$

The spatial difference of radon concentration that exists between the surface ($I=0$) and the underground induces a diffusive radon flow towards the surface. Also an advective radon flow can be initiated if a spatial air pressure difference exists in the subsurface. Nazaroff (1992) discussed possible origins for an air flow field in the underground. He concludes that the advective flux is mostly due to temperature differences between the free surface and the building, due to wind or due to ventilation and heating inside the house.

Considering these transport mechanisms, the rate of change of radon concentration in soil pore air can be described by the general transport equation:

$$\frac{\partial I}{\partial t} = \underbrace{\nabla D \nabla I}_{\text{Diffusion}} - \underbrace{v \nabla I}_{\text{Advection}} \underbrace{-\lambda I}_{\text{Decay}} + \underbrace{G}_{\text{Generation}} \qquad (2)$$

Mass transport (i.e. air flow) in the soil can be described by Darcy's law, if the value of the Reynolds number is smaller than about 4. The mean air velocity can be derived by a scaling with the porosity to:

$$\frac{1}{\epsilon}\cdot\left(\frac{k}{\mu}\nabla P\right) = v \qquad (3)$$

For the pressure field the Laplace-equation can be assumed:

$$\nabla\left(\frac{k}{\mu}\nabla P\right) = 0 \qquad (4)$$

Numerical tool

During the last four years the new finite element code "FRACTure" has been developed (Kohl, 1992). It was originally conceived to study the response of a hot fractured medium to a forced injection of cold fluid. For a correct treatment of this problem a full coupling between hydraulic, thermal and elastic processes had to be implemented in the code. The program's name "FRACTure" therefore is a acronym for its coupling mechanisms: **F**low, **R**ock **A**nd **C**oupled **T**emperature effects. During the code development, it was always kept in mind that FRACTure should be flexible to serve as a general tool for the simulation of

various coupled processes in geoscience.

Figure 1 shows the structure of FRACTure. New physical processes (for example radon transport or mass transport) are linked as "element-types" (i.e. a set of subroutines) to the program kernel. The kernel drives the new subroutines and actualizes the coupling order. A detailed description of the code can be found in Kohl (1992).

As the code was already used for different geophysical purposes (geoelectrical and hydraulic simulations), it was intended to apply it for the simulation of radon flow in the subsurface too. The existing structure of the code almost fitted in the needed structure for the radon transport simulation: no changes were necessary for the mass transport equation, since the air flow is described with a Darcy constitutive law as is the originally implemented water flow in aquifers. Furthermore, the coupling logic of a hydro-thermal regime corresponds exactly to the requirements of radon transport. According to eq. (2) the coupling from mass transport to radon transport consists of the transfer of an air velocity field that serves as advective term in the radon elements.

The new designed 1-D, 2-D and 3-D radon element types look similar to the already existing thermal element types. They only differ by an additional calculation of the interactions that are due to the radioactive decay. Once this term was included in the new radon elements, it had to be verified against an analytical solution.

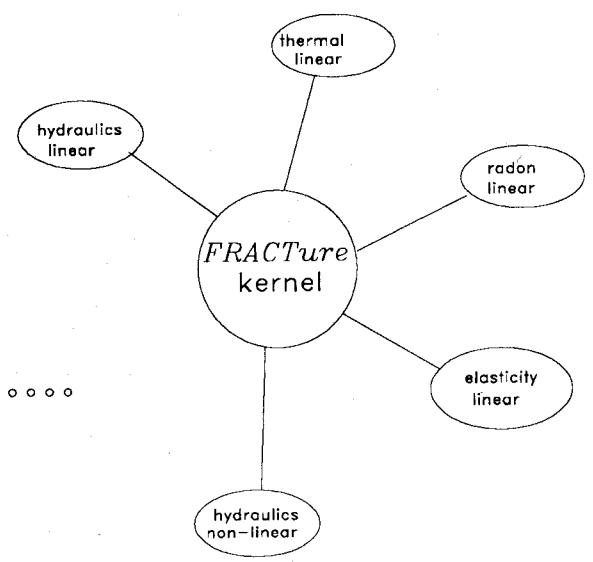

Fig. 1. Structure of FRACTure. Different element types can be linked to the program's kernel.

Verification of radon elements

Telford (1983) presented a model of one-dimensional radon transport from the underground to the surface. At the lower end a boundary condition with a constant radon concentration is assumed. At the surface the concentration is held at zero (i.e. radon is allowed to leave the model domain here). Between the upper and the lower end no radon is generated. A diffusive flux will establish due to the concentration difference. Also an advective flux is admitted, with an upward directed air-velocity field. Telford (1983) gave an analytical solution for this problem:

$$I = I_0 \cdot \exp\left[\frac{(l-r)v}{2D}\right] \cdot \frac{\sinh\left(r \cdot \sqrt{\frac{v^2}{4D^2}+\frac{\lambda}{D}}\right)}{\sinh\left(l \cdot \sqrt{\frac{v^2}{4D^2}+\frac{\lambda}{D}}\right)} \quad (5)$$

The boundary conditions can be easily derived from eq. (5); at the lower end with $r=l$ the concentration is I_0 and at the surface ($r=0$ m) the concentration is 0 Bq m^{-3}. The radon element types were verified against this analytical solution. A 10 m deep domain was assumed in vertical direction. The numerical model was discretized into equally spaced 50 cm lagrangian elements. The model parameters were taken as $D=1.0\times10^{-6}$ m^2/s, $v=1.0\times10^{-6}$ m/s; the decay constant of radon is 2.1×10^{-6} s^{-1}. The result of the verification is shown in Fig. 2. It contains comparisons for three different problems, each with differently activated mechanisms:

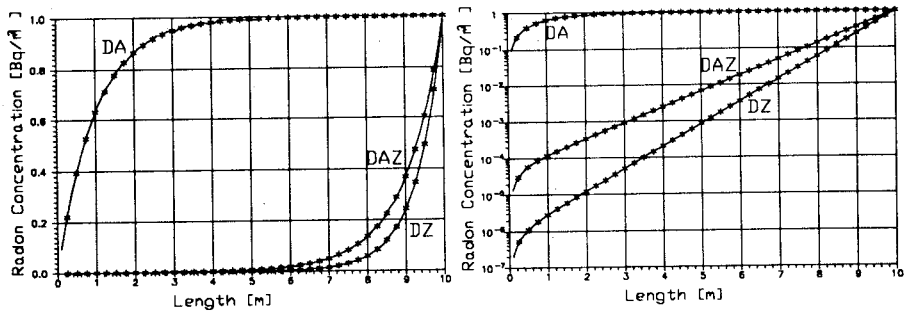

Fig. 2. Comparison of steady state concentrations for three cases each with differently activated mechanisms: Diffusion–Advection–Decay (*DAZ*), Diffusion–Advection (*DA*), and Diffusion–Decay (*DZ*). The numerical results are shown by an asterisk, the analytical solution by a straight line. The logarithmic scale (right) shows a better resolution at low concentrations.

(1) Diffusion–Advection–Decay
(2) Diffusion–Advection
(3) Diffusion–Decay

An excellent agreement between the numerical and the analytical calculation for all three case-problems can be seen. For a better representation of the small values a second figure was plotted with a logarithimcally scaled concentration axis. The deviations are far below 1%. The accuracy of the numeric model deteriorates with a coarser grid size. For example the deviations for element sizes of 1 m already are about 8%.

Simulations

Background and overview

In order to demonstrate the capabilities of the new radon elements in FRACTure, we have chosen a model that is close to the simulation of Loureiro et al. (1990) but that considers some special aspects of Swiss mountain dwellings. In a radon survey on selected sites in Switzerland high indoor radon concentrations were measured (up to 10,000 Bq/m^3 - see Medici, 1992; Medici and Rybach, 1994-this volume). In these areas the radon may originate from greater depth due to the high permeabilities of the underground. Furthermore, the buildings on these sites often do not have any foundation of concrete. The underground below the cellar then is only compressed soil, or sometimes even outcropping rock with large open joints. Thus there is only a low resistivity for the diffusive or advective radon flux to the buildings. These extremly exposed buildings are often located in mountain areas on Quaternary deposits or on karstic Jurassic limestones.

For the simulation of radon flux into the cellar of a building, a cylindrical model was assumed. The geometry was carefully chosen in order to avoid any boundary effects. Several different models have shown that a depth extension of about 15 m and a lateral extension of 20 m is sufficient. The underground structure of the building is assumed to have a depth of 1.5 m and a foundation thickness of 0.3 m. The radius of the building is 5 m. The geometry of the house and the spatial discretisation of the underground are shown in Fig. 3.

The radon concentration at the free surface is assumed to be zero. The other domain borders have a no flow boundary condition. Since the model cannot predict the air exchange in the building that strongly depends upon human influences (ventilation habits, etc.), the concentration in the building is generally calculated via the rate of radon inflow and an air exchange rate:

$$I_h = \frac{J_{tot}}{V_h \cdot (\lambda + L)} \qquad (6)$$

Two transport mechanisms of radon entry into

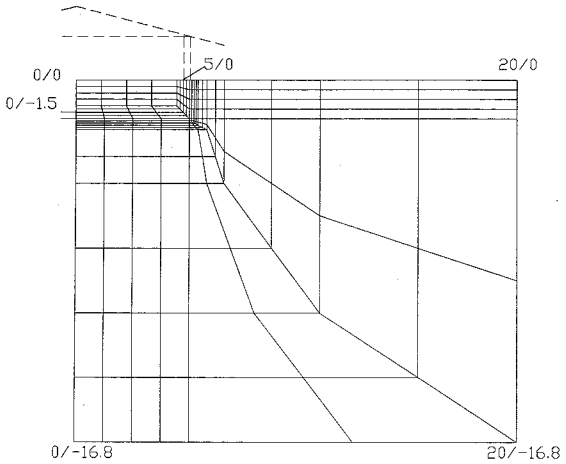

Fig. 3. Discretisation of cylindrical model domain with shilouette of building. A total extension of 20 m laterally and 16.8 m vertically was assumed. For avoiding numerical instabilities the smallest element sizes were taken near walls and foundation.

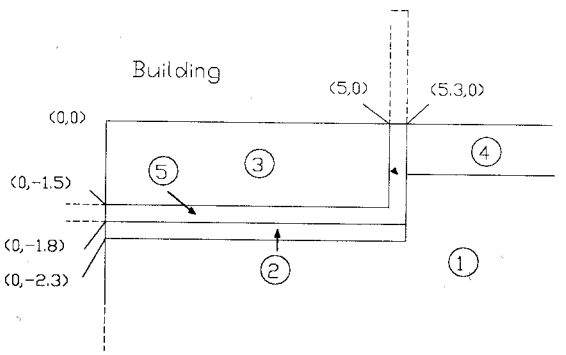

Fig. 4. Model subdivision for different material properties: undisturbed underground (material *1*), compressed underground (*2*), air in the building (*3*), vegetable soil (*4*) and wall/foundation (*5*).

the building are admitted: diffusion due to a radon concentration difference between the surface and the underground and advection due to an air pressure difference between the free surface and the building. This pressure difference is produced by a thermal gradient that always exists between the interior of the building and the outdoor surface. It initiates an air flow from the surface through the soil to the foundation of the building.

The air pressure can be described with the ideal gas law. According to Nazaroff (1992), a temperature difference of 20°C and a vertical distance to the undisturbed pressure of 3 m yields a pressure difference of 2.6 Pa. In our simulation the differential pressure between the surface and the building's foundation has been varied between −5 and −10 Pa. Since barometric and other transient influences cause pressure differences in the same order of magnitude, even values below −10 Pa seem reasonable. The thermally induced pressure difference is therefore a base value.

Material parameters

In several radon surveys (see for example Medici, 1992) it was suggested that in buildings with very high radon concentration the advective radon flux is the most important driving mechanism during the periods when the highest radon concentrations were observed. Therefore, in the steady state simulations presented here the parameter variations concerned advection only. So the rate of radon entry into houses was calculated as a function of the soil gas permeability and the driving advective pressure difference. Figure 4 shows the subdivision of the model into five different material sets: undisturbed underground, compressed soil, air in the building, vegetable soil and foundation. A selection of the material properties used in the simulations is given in Table 1, the values of other properties are assumed not to be material dependant and are given in Appendix 1. In order to clarify the effects of every parameter change, the material properties in the simulations are kept as homogeneous as possible. Different properties were only assumed between air and underground material.

The gas permeability that affects only the advective flux has been varied in a range from 10^{-14} m^2 to 10^{-11} m^2 (in geological terminology, the permeability ranges from sandy clay to clean sand).

TABLE 1

Material properties of radon transport simulation

	Undisturbed underground	Compressed underground	Air	Vegetable soil	Wall and foundation
Eff. Diffusivity [m^2/s]	10^{-6}	10^{-6}	1.3×10^{-5}	10^{-6}	10^{-6}
Porosity	0.4	0.4	1	0.4	0.4
Permeability [m^2]	Varying	Varying	∞	Varying	Varying

Discussion

As expected the simulations demonstrate that the source region of indoor radon extends only over a few meters below and around the building. In Figs. 5–7 the radon concentration field and the air pressure field in the underground are shown for low permeabilities with a pressure difference of -5 Pa and for high permeabilities with pressure differences of -5 and -10 Pa, respectively. The radon concentration is shown in shaded isolines, the appropriate values can be identified by a scale. The pressure field is also presented in the same figures as black labeled isolines. The label corresponds to the pressure value in Pa.

The undisturbed radon concentration is reached in all calculations performed at least at 3 m below the building. The radon level in that undisturbed region agrees with the theoretical value given by Telford (1983):

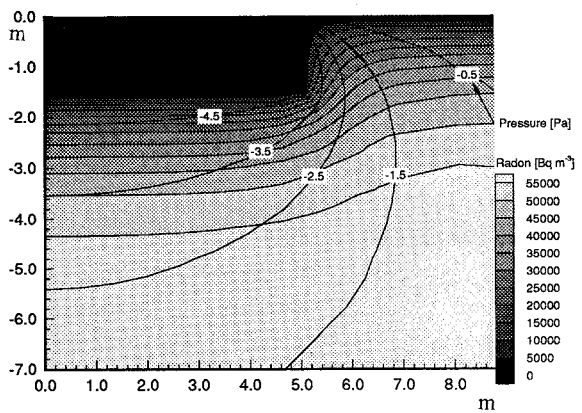

Fig. 5. Simulation with 5 Pa pressure difference and an underground permeability of 10^{-14} m^2. The radon concentration is shown in shaded isolines, the appropriate values can be identified by the scale at right. The values of the differential air pressure are indicated as labels on the black isolines.

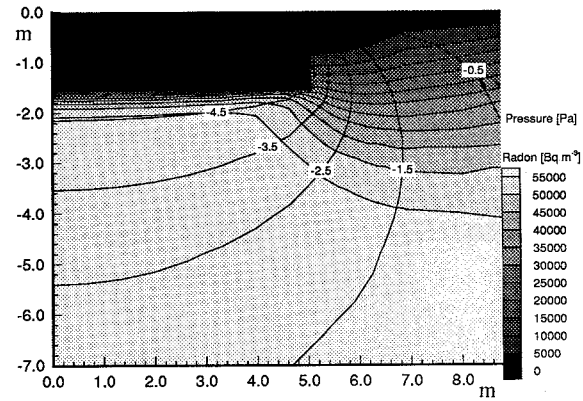

Fig. 6. Simulation with 5 Pa pressure difference and an underground permeability of 10^{-11} m^2.

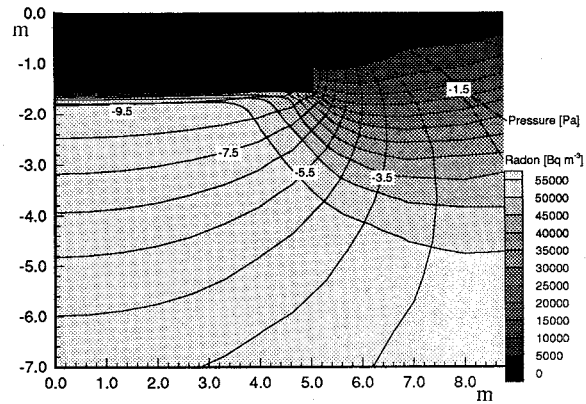

Fig. 7. Simulation with 10 Pa pressure difference and an underground permeability of 10^{-11} m^2.

$$I_{\text{undisturbed}} = f\rho_s A_{Ra}(1-\epsilon)/\epsilon$$
$$= 59{,}650 \text{ Bq m}^{-3} \quad (7)$$

Comparison of these figures shows, that the radon flow into buildings is strongly influenced by advection. In a low permeable underground (Fig. 5) the perturbation in the radon concentration field created by the building can be well recognized. The advective effect is very small; the stratification of radon is mainly due to the diffusive transport. Table 2 shows that for permeabilities of 10^{-14} m^2 a twofold pressure increase produces only an insignificantly small increase of indoor radon content. However, at higher permeabilities advection starts to play a dominant role in radon transport. Pressure increase then produces a strong increase in radon content in the building. Figures 6 and 7 show how the air flow field for permeabilities of 10^{-11} m^2 forces the radon to the domain just below the building. The indoor radon content in this case already might affect human health.

TABLE 2

Permeability and pressure dependent indoor radon concentrations (in Bq/m^3)

	10^{-14} [m^2]	10^{-13} [m^2]	10^{-12} [m^2]	10^{-11} [m^2]
5 Pa	92	95	137	374
10 Pa	94	104	175	441

Conclusions and outlook

It is shown that FRACTure is a versatile tool that can be used for the simulation of radon transport. The significance of advection as driving mechanism for indoor radon content that was expected by several radon surveys is now quantitatively proven.

FRACTure can be used also in considering countermeasures to mitigate radon risk. Several constructive measures like underfloor ventilation can be designed to reduce indoor radon levels. For the attempted radon reduction various scenarios can be calculated with the code FRACTure by taking into account the local ground properties and the materials and construction of the given building (see Table 1).

Still more work has to be done in the future for estimations of transient effects that are already known to be important. Another possible important source of underground air flow is the temperature difference due to natural thermal gradients in the subsurface and not only the indoor–outdoor temperature difference.

Acknowledgements

The computer code FRACTure was developed within the framework of the research project "Modelling of Energy Production from Hot Dry Rock Systems", financed by the Swiss National Energy Research Fund (NEFF). The authors would like to thank the program group RAPROS (Radon Programm Schweiz) and especially Prof. Dr. H.H. Loosli (Universität Bern) for continuous encouragement and support.
Contribution No. 763, Institute of Geophysics, ETH Zurich, Switzerland

Appendix 1

Notations

The values for the generally used parameters are given in parentheses

A_{Ra} [Bq/kg]	^{226}Ra content in soil (50 Bq/kg)
I [Bq/m^3]	Radon concentration
I_h [Bq/m^3]	Radon concentration in house
J_{tot} [Bq/m^{3}s]	Total radon inflow in house
D [m^2/s]	Effective diffusivity (2.0 m^2/s)
f	Emanation coefficient (0.3)
G [Bq/m^3 s]	Radon generation rate
k [m^2]	Permeability

l [m]	Length of domain in eq. (5) (10 m)
L [s^{-1}]	Air exchange rate ($1.4\times10^{-4}\ s^{-1}$)
P [Pa]	Pressure
r [m]	Distance from surface in eq. (5)
v [m/s]	Air velocity
V_h [m^3]	Volume of building
ϵ	Porosity
λ [s^{-1}]	Decay constant of ^{222}Rn ($2.1\times10^{-6}\ s^{-1}$)
μ [Pa s]	Dynamic viscosity of air (1.8×10^{-6} Pa s)
ρ_s [kg/m^3]	Density of soil grains (2650 kg m^{-3})

References

Andersen, C.E., 1992. Entry of Soil Gas and Radon into Houses, Risö Nat. Lab., Roskilde, Risö-R-623 (EN).

Kohl, T., 1992. Modellsimulation gekoppelter Vorgänge beim Wärmeentzug aus heissem Tiefengestein. Ph.D. Thesis. ETH Zürich, Nr. 9803, Zürich.

Loureiro, C. de O., Abriola, L.M., Martin, J.E. and Sextro, R.G., 1990. Three-dimensional simulation of radon transport into houses with basements under constant negative pressure. Environ. Sci. Technol., 24: 1338–1348.

Medici, F.V., 1992. Zusammenhänge zwischen lokaler Geologie und Radon-Konzentrationen in Wohnhäusern, Erste Ergebnisse aus der Schweiz. Ph.D. Thesis. ETH Zürich, Nr. 9931, Zürich.

Medici, F. and Rybach, L., 1994. Measurements of indoor radon concentrations and assessment of radiation exposure. J. Appl. Geophys., 31: 153–163, this volume.

Nazaroff, W.W., 1992. Radon transport from soil to air. Rev. Geophys., 30(2): 137–160.

Nazaroff, W.W. and Nero, A.V., 1988. Radon and its Decay Products in Indoor air. Wiley, New York, NY.

Nazaroff, W.W. and Sextro, R.G., 1989. Technique for measuring the indoor ^{222}Rn source potential of soil. Environ. Sci. Technol., 23(4): 451.

Sögaard-Hansen, J. and Damkjær, A., 1987. Determining ^{222}Rn diffusion lengths in soils and sediments. Health Phys., 53(5): 445–459.

Telford, W.M, 1983. Radon mapping in the search for uranium. In: A.A. Fitch (Editor), Developments in Geophysical Exploration Methods, Vol. 4 Elsevier, Barking, pp. 155–194.